PERGAMON

International Journal of Heat and Mass Transfer 42 (1999) 2255–2267

International Journal of HEAT and MASS TRANSFER

A new application of successive approximation to radiative exchange among surfaces: direct and inverse problems

C.-Y. Wu*, S.-H. Wu

Department of Mechanical Engineering, National Cheng Kung University, Tainan, Taiwan 701, Republic of China

Received 17 February 1998; in final form 26 June 1998

Abstract

A technique based on a successive approximation method is proposed to solve direct and inverse problems of radiative exchange among surfaces. With the present technique, the radiative exchange can be formulated by an expression in terms of some integrals and the surface reflectivity. The integrals are independent of the reflectivity and can be obtained by only one calculating procedure, provided that the geometry is fixed. The Monte Carlo method and the quadrature method are applied to perform the integration. Thus, after obtaining the integrals, the direct solutions for the values of the reflectivity of some concern to us can be readily obtained by substituting those values into the expression. Moreover, employing the present technique, we can solve an inverse problem estimating the surface reflectivity without solving the associated direct problem repetitively. Results of the three examples considered show that both of the direct and inverted results are in good agreement with the benchmark solutions.

Nomenclature

a channel radius
A area of enclosure surface
A_p a finite surface
B_0, B_m^s, B_m^d coefficients in equation (20), defined by equations (21)–(23)
$B_{m_1m_2}^0, B_{m_1m_2}^1, B_{m_1m_2}^2$ coefficients in the successive approximation of Q_d^-, see equation (24)
c_r function defined by equation (13)
c_v function defined by equation (18)
C tube center-to-center distance
D tube diameter or sphere diameter
E emissive power
g function describing the geometry of enclosure surface, see equation (A3)
H row separation distance
I radiation intensity
$\mathscr{K}$ integral operator, defined in equation (5)
L channel length
M degree of the polynomial for I or Q^-
$\hat{n}$ unit normal vector
N bundle number
Q radiative transfer rate
$\bar{r}$ position vector
R_f apparent reflectivity
$\hat{s}$ unit vector along a given direction
T temperature
T_r apparent transmissivity
U_0, U_m^s, U_m^d coefficients in equations (9) and (15), defined by equations (10)–(12) and (16)–(17)
V driving term, defined in equation (2)
W side length of a unit cell.

Greek symbols
ε emissivity
θ polar angle
ρ reflectivity
$\hat{\rho}$ inverted ρ
$\hat{\sigma}(\hat{\rho})$ estimator of the standard deviation of $\hat{\rho}$
μ cosine of polar angle
Ω solid angle.

Subscripts
b blackbody
d diffuse
i incoming
o external, or from outside
s specular

* Corresponding author. Fax: 00886 6 235 2973

0017–9310/99/$ - see front matter
PII: S0017–9310(98)00317–2

tr transmitted through a channel
λ at a given wavelength.

Superscripts
− entering opaque surface or leaving the enclosure
d diffuse
s specular.

1. Introduction

Radiative exchange of thermal energy among surfaces separated by vacuum or a nonparticipating medium plays an important role in many applications [1, 2]. Since thermal radiation is a long-range phenomenon, in order to make a radiative energy balance we always need to consider a complete enclosure consisting of real surfaces of known reflectivity and temperature (or flux) and/or imaginary surfaces (openings) over which the entering radiation is specified [3]. The radiative exchange of thermal energy among surfaces in nature is governed by the integral equation of radiation intensity [3]. For this reason, it is important to understand the mathematical character of the integral equation and the behavior of its solution. Since the radiative exchange among surfaces is determined by the surface reflectivity, the geometry and the distribution of temperature (or heat flux) of real surfaces and entering radiation through openings, the integral equation governing the physical process is also determined by the three factors. In this work, we call the third factor the driving term of the integral equation. In a lot of situations, we need to consider the variation of surface radiative exchange with respect to the reflectivity, as the geometry and the driving term are fixed. Based on observation and deliberation on the successive approximation [2], one of the most popular solution methods for integral equations, we find that for a rather large class of problems the surface reflectivity can be assumed constant or piecewise constant, and can be brought outside the integrals of the governing equation as well as the solutions obtained by the successive approximation. Once the integrals independent of the surface reflectivity are evaluated, the successive approximation solution becomes an algebraic expression in terms of the surface reflectivity. In other words, the variation of surface radiative exchange with respect to the reflectivity can be readily found by substituting the various values of the reflectivity into the algebraic expression without re-calculating the integrals. This feature of the successive approximation solution can enhance the efficiency, especially when the integration involved is time-consuming and laborious. Therefore, in this work, we aim at developing the new application of the successive approximation to the problems, for which the solutions for various values of the reflectivity are desired. This family of problems includes, among others, the inverse problem of estimating the reflectivities of surfaces of known geometry for the case with a given driving term. The present technique is promising for this family of problems, because it can generate direct or inverse solutions without repeating time-consuming integration.

To evaluate the coefficients of the algebraic expression in terms of the surface reflectivity, we adopted the reverse Monte Carlo method (RMC) [4, 5] and the quadrature method (QM) [6] to perform multiple integrations. The present technique needs only a single calculating procedure to generate the expression for various values of the surface reflectivity. Then, to demonstrate the present technique, three examples, thermal radiation transmitted through a cylindrical channel, radiative exchange in a packed sphere system and radiative transfer from an infinite plane to rows of parallel tubes of infinite length, are considered in Section 4. To assess the present technique, comparisons are made of the present results and the results available in the literature.

Both direct and inverse solutions are considered in the three examples. However, we put more emphasis on inverse solutions because of the feature of the present technique. That is, if the radiative intensity, or flux, or transfer rate on a real surface or an opening has been measured, the surface reflectivity can be estimated by applying a root-finding method to the algebraic equation of the surface reflectivity rather than by solving direct surface radiation exchange iteratively as done in many other methods for inverse problems. A few reports on the estimation of the distribution of surface temperature have been presented recently [7–12], while work on the estimation of a surface radiative property seems to be rare. Therefore, we apply the present technique to the inverse problems of radiative exchange among surfaces, where the surface reflectivity is to be estimated. In the three examples, we estimate the surface reflectivity of either simple or complicated enclosures, including cases with piece-wise constant reflectivity. The effects of geometric sizes and measurement errors on the inverted results are examined for various values of the surface reflectivity.

2. Analysis

The enclosure model is adopted here to describe the physical process of radiative exchange among surfaces in the absence of a participating medium. Consider an arbitrary enclosure composed of real surface and/or imaginary surfaces (openings), through which external irradiation may enter the enclosure, as shown in Fig. 1. The real surfaces are emitting, absorbing and reflecting, while the imaginary ones can be regarded as non-participating. The radiation intensity I leaving an infinitesimal surface element dA defined by a position vector

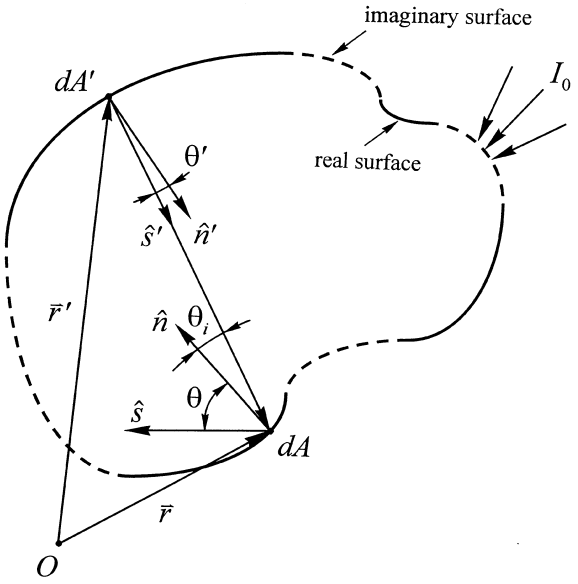

Fig. 1. The geometry of an enclosure.

$\bar{r}$ into the direction $\hat{s}$ can be described by the integral equation

$$I(\bar{r},\hat{s}) = V(\bar{r},\hat{s}) + \int_{2\pi} \rho''(\bar{r},\hat{s}',\hat{s}) I(\bar{r},\hat{s}') \mu_i \, d\Omega_i, \quad \hat{n}\cdot\hat{s} > 0 \tag{1}$$

where $\rho''(\bar{r},\hat{s}',\hat{s})$ denotes the bi-directional reflection function of dA for incident direction $\hat{s}'$ and leaving direction $\hat{s}$, $d\Omega_i = dA' \cos\theta'/|\bar{r}-\bar{r}'|^2$, $\mu_i = \cos\theta_i = (-\hat{s}')\cdot\hat{n}$ with $\hat{n}$ denoting the unit normal vector at dA, as shown in Fig. 1, and $V(\bar{r},\hat{s})$ the driving term defined by

$$V(\bar{r},\hat{s}) = \begin{cases} \varepsilon'(\bar{r},\hat{s}) I_b(\bar{r}), & \text{if } \bar{r} \text{ is located on a real surface} \\ I_o(\bar{r},\hat{s}), & \text{if } \bar{r} \text{ is located on an imaginary surface} \end{cases} \tag{2}$$

with $\varepsilon'(\bar{r},\hat{s})$ denoting the directional emissivity of dA, $I_b(\bar{r})$ the blackbody intensity, and $I_o(\bar{r},\hat{s})$ the intensity of entering radiation in the direction $\hat{s}$ at dA. The driving term is due to emission of a real surface or entering radiation through an opening, and $I_b(\bar{r})$ can be related to the local surface temperature $T(\bar{r})$ through Planck's law. The integral term of equation (1) is the contribution of reflected radiation on a real surface or identically zero, because $\rho''(\bar{r},\hat{s}',\hat{s}) = 0$ for an imaginary surface. Besides, a subscript λ denoting dependence on radiation wavelength has been dropped for simplicity. Hence, the above governing equation of intensity can be applied to describing monochromatic or gray-surface-property radiative exchange.

In the absence of a participating medium, the incident intensity at $\bar{r}$ along $\hat{s}'$ is equal to the leaving intensity at $\bar{r}'$ along $\hat{s}'$,

$$I(\bar{r},\hat{s}') = I(\bar{r}',\hat{s}') \tag{3}$$

$\bar{r}'$ in equation (3) defines the location, where the incident radiation originates from emission and reflection or from entering radiation. Besides, $\bar{r}'$ is determined by $\bar{r}$, $\hat{s}'$ and the geometry of the enclosure, as shown in Fig. 1.

Combining equations (1) and (3), we obtain

$$I(\bar{r},\hat{s}) = V(\bar{r},\hat{s}) + \int_{2\pi} \rho''(\bar{r},\hat{s}',\hat{s}) I(\bar{r}',\hat{s}') \mu_i \, d\Omega_i, \quad \hat{n}\cdot\hat{s} > 0 \tag{4}$$

If the reflectivity, the geometrical shape and the driving term (T for all real surfaces and I_o for all imaginary surfaces) are completely specified for all surfaces of the enclosure, we can find I by solving equation (4). Equation (4) in essence is a Fredholm integral equation of the second kind. This is shown in the Appendix.

To abbreviate mathematical expression, we introduce an integral operator $\mathscr{K}$, defined by

$$\mathscr{K}[I](\bar{r},\hat{s}) \equiv \int_{2\pi} \rho''(\bar{r},\hat{s}',\hat{s}) I(\bar{r}',\hat{s}') \mu_i \, d\Omega_i \tag{5}$$

Then, equation (4) reduces to

$$I(\bar{r},\hat{s}) = V(\bar{r},\hat{s}) + \mathscr{K}[I](\bar{r},\hat{s}) \tag{6}$$

If we replace I under the integral sign of equation (6) with equation (5) by an initial approximation $I^{(0)}$, equation (6) determines an approximation for the radiation intensity leaving an opaque surface

$$I^{(1)}(\bar{r},\hat{s}) = V(\bar{r},\hat{s}) + \mathscr{K}[I^{(0)}](\bar{r},\hat{s}) \tag{7}$$

Then, the higher order approximation for I can be obtained by substituting the current approximation into the right-hand-side of equation (6). Repeating this procedure, we obtain the infinite series solution

$$I(\bar{r},\hat{s}) = V(\bar{r},\hat{s}) + \sum_{m=1}^{\infty} \mathscr{K}^m[V](\bar{r},\hat{s}) \tag{8}$$

Obviously, the expression of I is a series of multiple integrations of the driving term, and $\mathscr{K}^m[V](\bar{r},\hat{s})$ for $m \geqslant 1$ represents the contribution of radiation for m-time reflections. In practice, the reflectivities of real surfaces of the considered enclosure are less than one, or the real surface reflectivities are unity but the enclosure has one opening at least. Thus, radiation may be absorbed by real surfaces or leave the enclosure through openings after several reflections, so the contribution of m-time reflections approaches zero as m becomes infinite. Hence, the series in equation (8) converges and the series may be truncated after a specific term, say $m = M$, in actual computation. Then, the truncated expression of equation (8) is a successive approximation solution for $I(\bar{r},\hat{s})$. Besides, it is noticed that the influence of the geometry and the surface reflectivity on I is coupled through the integral operator $\mathscr{K}$.

In many engineering applications, the entire enclosure surface can be assumed to be composed of a finite number of discrete surfaces over which the radiative properties are uniform. Furthermore, we may divide the solid angle domain 2π into discrete solid angle elements such that the bi-directional reflection function can be assumed constant within each discrete solid angle element and may vary from element to element. By increasing the number of discrete surfaces and refining the size of the solid angle elements, the actual distribution of the bi-directional reflection function can be approximated to any degree of accuracy. Then, with the piece-wise constant approximation, the surface reflectivity can be brought outside the integrals of equation (8). Hence, the resulting integrals of the successive approximation solution depend on both the geometry and the driving term, but are independent of the surface reflectivity. Once the integrals are evaluated, the successive approximation solution reduces to an algebraic expression in terms of the surface reflectivity. When the geometry and the driving term keep fixed and the surface reflectivity is changed alone, the surface radiative exchange for various values of the reflectivity can be readily obtained by substituting the values of the reflectivity into the algebraic expression without re-evaluation of the time-consuming integrals. To exemplify the present technique clearly, we assume that the surface reflection is either diffuse or specular and the surface emission is negligible or absent. From equation (2), it is readily found that either the entering radiation or the emission plays the role of driving term, and so the present technique can be employed to solve problems with surface emission. Moreover, the present technique can be extended to cases with more complex reflectivity distributions, provided that the surface reflectivity can be approximated by a piece-wise constant function.

First, we consider the specular reflection case. When the real opaque surfaces of the enclosure have a uniform specular reflectivity ρ_s independent of the incoming direction, ρ_s can be brought outside the integral defined by equation (5). Then, the truncated expression of equation (8) becomes

$$I(\bar{r},\hat{s}) = U_0(\bar{r},\hat{s}) + \sum_{m=1}^{M} \rho_s^m U_m^s(\bar{r},\hat{s}) \tag{9}$$

where

$$U_0(\bar{r},\hat{s}) = [1-c_r(\bar{r})]I_o(\bar{r},\hat{s}) \tag{10}$$

$$U_1^s(\bar{r},\hat{s}) = c_r(\bar{r})U_0(\bar{r}',\hat{s}_s') \tag{11}$$

$$U_m^s(\bar{r},\hat{s}) = c_r(\bar{r})U_{m-1}^s(\bar{r}',\hat{s}_s') \tag{12}$$

for $2 \leqslant m \leqslant M$, and

$$c_r(\bar{r}) = \begin{cases} 1, & \text{if } \bar{r} \text{ is located on a real surface} \\ 0, & \text{if } \bar{r} \text{ is located on an imaginary surface} \end{cases} \tag{13}$$

Here, $\hat{s}$ and $\hat{s}_s'$ are the directions after and before the specular reflection occurring at dA, respectively; that is, they obey the specular reflection law

$$\hat{s} = \hat{s}_s' + 2|\hat{s}_s' \cdot \hat{n}|\hat{n} \tag{14}$$

Next, we consider the case in which the real opaque surfaces are diffusely reflecting and have a uniform reflectivity ρ_d. Then the truncated expression of equation (8) reduces to

$$I(\bar{r},\hat{s}) = U_0(\bar{r},\hat{s}) + \sum_{m=1}^{M} \rho_d^m U_m^d(\bar{r}) \tag{15}$$

where

$$U_1^d(\bar{r}) = \frac{1}{\pi} c_r(\bar{r}) \int_{2\pi} U_0(\bar{r}',\hat{s}')\mu_i \, d\Omega_i = c_r(\bar{r}) \int_A c_v(\bar{r}';\bar{r}) U_0(\bar{r}',\hat{s}') \frac{\mu_i \mu'}{\pi|\bar{r}-\bar{r}'|^2} dA' \tag{16}$$

$$U_m^d(\bar{r}) = \frac{1}{\pi} c_r(\bar{r}) \int_{2\pi} U_{m-1}^d(\bar{r}')\mu_i \, d\Omega_i = c_r(\bar{r}) \int_A c_v(\bar{r}';\bar{r}) U_{m-1}^d(\bar{r}') \frac{\mu_i \mu'}{\pi|\bar{r}-\bar{r}'|^2} dA' \tag{17}$$

for $2 \leqslant m \leqslant M$, with $\mu' = \cos\theta' = \hat{s}' \cdot \hat{n}'$, as shown in Fig. 1, and

$$c_v(\bar{r}';\bar{r}) = \begin{cases} 1, & \text{if } dA' \text{ can be seen from } dA \\ 0, & \text{if } dA' \text{ cannot be seen from } dA \end{cases} \tag{18}$$

Here, $\hat{s}'$ can be expressed by $\bar{r}$ and $\bar{r}'$, as shown by equation (A2), and we have transformed the solid angle integrals into surface integrals.

If the enclosure consists of diffusely reflecting surfaces where the local temperature or heat flux is specified, the above formulation in terms of leaving intensity from a surface element can be readily transformed to that in terms of local radiosity. The equation of radiosity is still a Fredholm integral equation of the second kind [2].

We are often interested in finding the incident radiative transfer rate for a finite surface A_p of the enclosure. This quantity is defined by

$$Q^- = \int_{A_p} \int_{2\pi} I(\bar{r},\hat{s}')\mu_i \, d\Omega_i \, dA \tag{19}$$

Substituting equation (3) and the successive approximation of $I(\bar{r}',\hat{s}')$ into equation (19), we can express the incident radiative transfer rate as

$$Q_\alpha^- = B_0 + \sum_{m=1}^{M} B_m^\alpha \rho_\alpha^m \tag{20}$$

for α = s or d, where

$$B_0 = \int_{A_p} \int_{2\pi} U_0(\bar{r}',\hat{s}')\mu_i \, d\Omega_i \, dA = \int_{A_p} \int_A c_v(\bar{r}';\bar{r}) U_0(\bar{r}',\hat{s}') \frac{\mu_i \mu'}{|\bar{r}-\bar{r}'|^2} dA' \, dA \tag{21}$$

$$B_m^{\mathrm{s}} = \int_{A_p}\int_{2\pi} U_m^{\mathrm{s}}(\bar{r}',\hat{s}')\mu_{\mathrm{i}}\,\mathrm{d}\Omega_{\mathrm{i}}\,\mathrm{d}A \tag{22}$$

$$B_m^{\mathrm{d}} = \int_{A_p}\int_{2\pi} U_m^{\mathrm{d}}(\bar{r}')\mu_{\mathrm{i}}\,\mathrm{d}\Omega_{\mathrm{i}}\,\mathrm{d}A = \int_{A_p}\int_{A} c_v(\bar{r}';\bar{r})\,U_m^{\mathrm{d}}(\bar{r}')\frac{\mu_{\mathrm{i}}\mu'}{|\bar{r}-\bar{r}'|^2}\,\mathrm{d}A'\,\mathrm{d}A \tag{23}$$

for $1 \leqslant m \leqslant M$.

It is worth pointing out that (i) the right-hand-side of equation (9), (15) or (20) is a polynomial of ρ_α, (ii) the coefficients of the polynomial are multiple integrations of the driving term, and (iii) the coefficients are independent of the surface reflectivity if the surface emission is negligible or absent. As the surface emission is present, the emissivity is related to the constant surface reflectivity through Kirchhoff's law and can also be brought outside the integrals of the driving term. Then, an additional factor $1-\rho_\alpha$ appears and the resulting expression is also an algebraic expression in terms of ρ_α. For example, if the enclosure considered consists of imaginary surfaces and two opaque diffusely reflecting surfaces with reflectivities $\rho_{\mathrm{d}1}$ and $\rho_{\mathrm{d}2}$, the successive approximation of Q_{d}^- may be expressed as

$$Q_{\mathrm{d}}^- = \sum_{m_1=0}^{M_1}\sum_{m_2=0}^{M_2} B^0_{m_1m_2}\rho_{\mathrm{d}1}^{m_1}\rho_{\mathrm{d}2}^{m_2} + (1-\rho_{\mathrm{d}1})\sum_{m_1=0}^{M_1}\sum_{m_2=0}^{M_2} B^1_{m_1m_2}\rho_{\mathrm{d}1}^{m_1}\rho_{\mathrm{d}2}^{m_2} + (1-\rho_{\mathrm{d}2})\sum_{m_1=0}^{M_1}\sum_{m_2=0}^{M_2} B^2_{m_1m_2}\rho_{\mathrm{d}1}^{m_1}\rho_{\mathrm{d}2}^{m_2} \tag{24}$$

with the coefficients $B^0_{m_1m_2}$s, $B^1_{m_1m_2}$s and $B^2_{m_1m_2}$s representing appropriate integrals of the given I_{o} and I_{b}. Having obtained $B^0_{m_1m_2}$s, $B^1_{m_1m_2}$s and $B^2_{m_1m_2}$s, we can evaluate Q_{d}^- for various values of $\rho_{\mathrm{d}1}$ and $\rho_{\mathrm{d}2}$ by substituting those values into equation (24), provided that the geometry and the driving term (I_{o} and I_{b}) are fixed. Using other existing methods, for example, the conventional Monte Carlo method in [13], we have to perform the whole solution procedure if $\rho_{\mathrm{d}1}$ and $\rho_{\mathrm{d}2}$ are changed. Therefore, the present technique is particularly suitable, not only for direct problems in which the radiative exchange for various values of the surface reflectivity is our concern, but also for the inverse problem estimating the surface reflectivity with known geometry and a given driving term. In the inverse problem, if the radiative transfer rate of a discrete surface is measured, the surface reflectivity can be found by applying a root-finding method to the algebraic expression of the radiative transfer rate rather than solving direct surface radiative exchange iteratively as done in many other methods for inverse problems.

If the surface reflectivity is described by more than one parameter, the number of radiative intensities, fluxes or transfer rates measured shall not be less than the number of the parameters. Then, the parameters describing the surface reflectivity can be estimated by a least squares minimization method or simultaneously solving the algebraic expressions of the measured radiative physical quantities.

3. Numerical methods

To illustrate the numerical methods for the evaluation of the coefficients of the polynomial of the surface reflectivity, we consider the expressions of Q^-, equations (20) and (24). The coefficients in the expressions of Q^- are the multiple integrations of the driving term. Although analytical integration can be performed for cases of very simple geometry, numerical methods are more feasible in general.

3.1. Reverse Monte Carlo method

In this work, we adopted the RMC [4, 5] originally developed to solve the radiative transfer in a participating medium, because it provides a better estimator for intensity, incident radiation or radiative flux at a point with a smaller random error than the conventional Monte Carlo method does. The basis of this method is the principle of reciprocity in radiative transfer theory [5], and the bundle tracing is in a time-reversed manner. The details have been described [5] and so they are not duplicated here.

When we employ the RMC to the simulation of the successive substitution procedure generating equations (9), (15), (20) or (24), we require that the value of the surface reflectivity shall not be specified in advance. To meet this requirement, we adopt the RMC with importance sampling. Dunn [14] applied the conventional Monte Carlo method with importance sampling to generating an expression in terms of the scattering albedo for the transmissivity or the reflectivity of an isotropically scattering slab. His results show that the importance sampling technique works very well, except that the resulting expression does not include the coefficients in explicit form.

In the bundle-tracing procedure of the RMC with importance sampling, when the traced bundle strikes a real surface element, we do not require to generate a random number to determine the interaction between the bundle and the struck surface element as is done in the original RMC, but force the bundle to be reflected to continue the tracing procedure. The tracing procedure stops when the bundle strikes an imaginary surface and we score the entering radiation at the imaginary surface element, or when the number of reflections that the bundle has undergone is more than a prescribed number. Before the ending of tracing a bundle, the total number

of reflections is scored for the entering radiation. If the surface emission is present, the local blackbody intensity should be scored for each strike, and the scores resulting from emission and those resulting from entering radiation shall be counted separately because the scores resulting from surface emission have to be multiplied by an additional factor $1-\rho_\alpha$. Hence, after N bundles are traced, the coefficient B_m^α can be estimated by the product of $\pi A_p/N$ and the sum of the scores for m-time reflections. Then, we can obtain the algebraic expression for Q^- in terms of the surface reflectivity.

3.2. Quadrature method

The QM employs a numerical quadrature to approximate an integral. When Q_d^- is evaluated by equation (20) with the coefficients in the surface integral form using the QM, the area integrations over the entire enclosure surface are first divided into the area integrations over real surfaces and those over imaginary surfaces. Each of the area integrations is approximated by a product quadrature formula. Then, for the diffuse reflection cases the values of U_0 and U_m^ds on all quadrature nodes can be evaluated by the recurrence relations, equations (16) and (17), and the coefficients B_0 and B_m^ds can be obtained by equations (21) and (23). For the specular reflection cases, the coefficients B_m^ss can be obtained in a similar way, while equations (10)–(12) can be treated by the ray tracing procedure. Similarly, the QM can be applied to the evaluation of Q_d^- by equation (24). Moreover, since the integrands of the integrals in the surface integral form often have integrable singularities or some low-order derivatives (usually the first derivative) of the integrands are singular, the subtraction technique stated in [6] is employed to improve the results of the QM in this work.

4. Examples

4.1. Radiative transfer through a cylindrical channel

The first example considered here is radiative transfer transmitted through a cylindrical channel of radius a and of length L, as shown in Fig. 2(a). The channel is exposed to a uniform diffuse radiative intensity I_d at its top end, and its bottom end is an opening free from external radiation. The inner lateral surface of the channel is assumed to be opaque, uniform, gray, cold (or non-emitting), reflecting and absorbing. To obtain the direct solution of the example, we apply the RMC with importance sampling to either specularly or diffusely reflecting cases and the QM to diffusely reflecting cases, while an analytical solution of the transmitted radiative transfer rate for the specular cases was presented by Rabl [15]. The analytical solution for the transmitted radiative transfer rate was given as

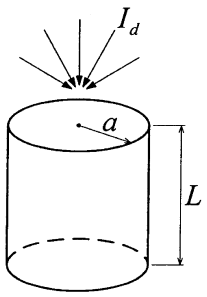

(a) a cylindrical channel

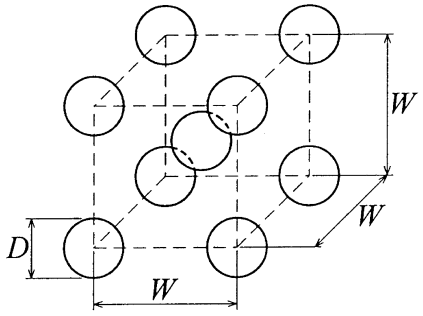

(b) spheres packed in a BCC arrangement

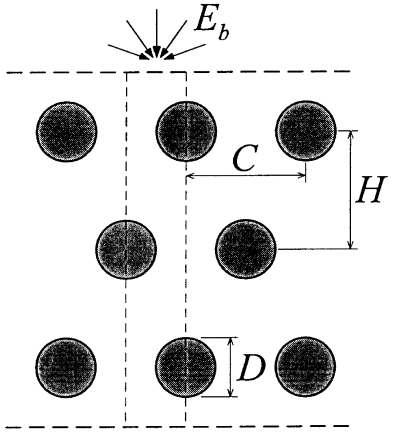

(c) rows of parallel tubes between two infinite planes

Fig. 2. The geometries of the examples considered.

$$\frac{Q_{\mathrm{tr}}}{\pi^2 a^2 I_{\mathrm{d}}} = 1 - \frac{L}{a}(1-\rho_s)^2 \sum_{n=1}^{\infty} \rho_{\mathrm{s}}^{n-1} \times \left\{ \left[1 + \left(\frac{L}{2na} \right)^2 \right]^{1/2} - \left(\frac{L}{2na} \right) \right\} \quad (25)$$

If only finite terms of the series in equation (25) are adopted, the exact solution reduces to a successive approximation. Results for the transmitted radiative transfer rate by the three methods are listed in Table 1. Comparison of the results shows very good agreement for various combinations of ρ_{s} or ρ_{d} and L/a.

The present RMC computation uses 10 000 000 bundles in each case. In all Tables presented in this work, the value just following each RMC result in parentheses is the estimator of the standard deviation of the result. The standard deviation can be viewed as an indicator of the magnitude of the random error inherent in the result. Observing the ratio of the indicator of random error to the transmitted rate shown in Table 1, we find that the performance of the RMC becomes better when L decreases or ρ_{α} increases.

Here, the QM adopts the Gaussian quadrature formulas. The QM results show convergence when we increase the number of nodes of the Gaussian quadrature, and the listed results in the bottom half of Table 1 are the convergent values. The value just following each QM result in parentheses is the node number of the Gaussian quadrature formula employed.

Next, we consider an inverse problem for the same geometry; the inverse problem estimates the lateral surface reflectivity of the cylindrical channel. To shorten the length of this report, here we consider only the diffusely reflecting case, while similar procedure can be applied to the specularly reflecting case. Provided that the transmitted radiative transfer is obtained by measurement and that the coefficients on the right-hand-side of equation (20) are evaluated by the RMC with importance sampling, the value of ρ_{d} can be readily estimated by finding the root of equation (20). Since the coefficients on the right-hand-side of the algebraic equation are all positive, the right-hand-side of the equation is a non-decreasing function for ρ_{d} varying in the [0, 1] interval. Then, the root of the algebraic equation in the [0, 1] interval is unique, and it can be easily solved by any conventional root-finding method, for example, Brent's method [16].

Here, we adopt the Q^- solved by the QM to simulate the required 'measured' Q^- on the bottom opening for a specified reflectivity of the lateral surface. The inverted results for diffuse reflectivity ($\hat{\rho}_{\mathrm{d}}$) are benchmarked against the specified values of ρ_{d} in the top half of Table 2, where the value just following each inverted result in the parentheses is the estimator of the standard deviation of $\hat{\rho}$, $\hat{\sigma}(\hat{\rho})$. The value of $\hat{\sigma}(\hat{\rho})$ can be viewed as an indicator of the magnitude of the random error inherent in $\hat{\rho}$, and the approach to obtain $\hat{\sigma}(\hat{\rho})$ has been described in [14]. Each inverted result in Table 2 is obtained by tracing $N = 500\,000$ bundles in the RMC computation for the coefficients B_0 and B_m^{d}s, and the value of M is the largest number of bundle reflections generated in the tracing procedure. In general, the difference between the exact value and the computed value of B_0 and B_m^{d} by the RMC decreases with the increase of the bundle number N, because the random error inherent in the Monte Carlo solution has order $N^{-1/2}$. Therefore, we may expect that the inverted results approach the exact reflectivity as N increases. Inverted results for a wide range of combinations of L/a and ρ_{d} have been checked, and the convergence tendency is confirmed by those inverted results.

As shown in the top half of Table 2, the inverted results by the RMC agree well with the exact values in most of the cases. Since there are no measurement errors within the 'measured' Q^-s, the differences between the inverted results and the exact values are almost totally due to the random error resulting from the finite samplings, and they are in the same order of magnitude as $\hat{\sigma}(\hat{\rho}_{\mathrm{d}})$, as

Table 1
The radiative transfer transmitted through a cylindrical channel with a specularly- or diffusely-reflecting lateral surface

		$Q_{\mathrm{tr}}/(\pi^2 a^2 I_{\mathrm{d}})$	
L/a	ρ_{s}	Analytical	RMC
0.1	0.1	0.9142	0.9142 (0.00008)
	0.5	0.9517	0.9517 (0.00005)
	0.9	0.9901	0.9901 (0.00001)
1.0	0.1	0.4285	0.4285 (0.00014)
	0.5	0.6387	0.6387 (0.00010)
	0.9	0.9111	0.9111 (0.00003)
10.0	0.1	0.0163	0.0163 (0.00003)
	0.5	0.0847	0.0847 (0.00005)
	0.9	0.5040	0.5040 (0.00008)
		$Q_{\mathrm{tr}}/(\pi^2 a^2 I_{\mathrm{d}})$	
L/a	ρ_{d}	QM	RMC
0.1	0.1	0.9094 (3)	0.9095 (0.00009)
	0.5	0.9280 (3)	0.9281 (0.00007)
	0.9	0.9474 (3)	0.9475 (0.00007)
1.0	0.1	0.4001 (5)	0.3998 (0.00015)
	0.5	0.4909 (5)	0.4907 (0.00014)
	0.9	0.6269 (5)	0.6268 (0.00014)
10.0	0.1	0.0101 (5)	0.0101 (0.00003)
	0.5	0.0129 (11)	0.0129 (0.00003)
	0.9	0.0508 (31)	0.0508 (0.00005)

Table 2
The inverted diffuse lateral surface reflectivities of cylindrical channels from the Q^-s with or without simulated measurement errors

			RMC	RMC with analytical evaluated B_o
L/a	ρ_d	$Q^-/(\pi^2 a^2 I_d)$	$\hat{\rho}_d$	
0.1	0.1	0.9094	0.1033 (0.0087)	0.1001 (0.0006)
	0.5	0.9280	0.5038 (0.0070)	0.5008 (0.0031)
	0.9	0.9474	0.9047 (0.0061)	0.9018 (0.0055)
1.0	0.1	0.4001	0.1029 (0.0035)	0.1002 (0.0003)
	0.5	0.4909	0.5028 (0.0023)	0.5009 (0.0010)
	0.9	0.6269	0.9022 (0.0015)	0.9010 (0.0013)
10.0	0.1	0.0101	0.1293 (0.0371)	0.1008 (0.0022)
	0.5	0.0130	0.5072 (0.0098)	0.5001 (0.0030)
	0.9	0.0508	0.9003 (0.0005)	0.9001 (0.0004)
L/a	ρ_d	Measurement error	$\hat{\rho}_d$	
1.0	0.1	−3.0%	0.0376 (0.0038)	0.0347 (0.0001)
		−1.0%	0.0815 (0.0036)	0.0788 (0.0002)
		+1.0%	0.1239 (0.0035)	0.1213 (0.0003)
		+3.0%	0.1648 (0.0033)	0.1623 (0.0004)
1.0	0.5	−3.0%	0.4473 (0.0024)	0.4453 (0.0009)
		−1.0%	0.4846 (0.0023)	0.4827 (0.0010)
		+1.0%	0.5206 (0.0022)	0.5188 (0.0010)
		+3.0%	0.5553 (0.0021)	0.5535 (0.0010)
1.0	0.9	−3.0%	0.8566 (0.0015)	0.8554 (0.0013)
		−1.0%	0.8873 (0.0015)	0.8861 (0.0013)
		+1.0%	0.9168 (0.0015)	0.9157 (0.0013)
		+3.0%	0.9454 (0.0014)	0.9442 (0.0013)

expected. Comparison among various cases shows that the performance of the present method for the cases of large L and small ρ_d is worse than that for the other cases. The performance of the present method degenerates, when the RMC used to evaluate B_0 and B_m^ds becomes inefficient or when the absolute value of $\partial Q^-/\partial \rho_d$ is small. The former includes the cases where B_0 is too small to be evaluated accurately by the RMC for a long tube and where the contribution of reflection to Q^- is small because of a low lateral surface reflectivity. It is found that B_0 can be integrated analytically for the present geometry. By integrating B_0 analytically and evaluating B_m^ds by the RMC, we may improve the results as shown in Table 2.

In most practical applications, the measured values always contain a few percent of error. Hence, we have to examine the effect of the measurement error on inverted results. In the bottom half of Table 2, we tabulate some inverted results for the Q^-s obtained by adding or subtracting 1.0 and 3.0% of their exact values for $L/a = 1.0$. The bottom half of Table 2 shows that the inverted results for the Q^-s with smaller simulated measurement errors are closer to the exact values than those with larger simulated measurement errors, and the inverted results from the Q^-s with 3.0% simulated measurement errors are still meaningful.

In this example, it takes 36 CPU s on a HP 715 workstation to invert 27 values of the diffuse surface reflectivity for a channel of $L/a = 1.0$ using 500 000 bundles. Since most of the CPU time is spent on the bundle-tracing procedure, the present inverse method requires almost as much CPU time as a direct solution procedure by the RMC with importance sampling. On the other hand, the others of inversion methods usually take several times the CPU of their direct solutions because of their iteration nature.

4.2. Radiative exchange in a packed sphere system

The second example considered is to solve the radiative exchange in a regularly packed sphere system. This problem has been viewed as a simplified model of radiative transfer in porous media [17–19], where the geometric dimensions of the pores within the porous media are so large that radiative transfer in the media can be treated in the geometric optics range. The present system consists of infinite horizontal layers of identical cold opaque large spheres packed in a BCC arrangement, as shown in Fig. 2(b), and the top of the packed system is exposed to a uniform diffuse radiation of intensity I_d, where D is the diameter of a sphere, and W is the side length of a unit cell. The surfaces of the spheres are assumed to be gray, absorbing and diffusely or specularly reflecting, and the reflectivity of the surfaces is constant. Besides, diffraction phenomenon is supposed to be negligible [17–19]. Then, radiative transfer in the packed system can be treated as surface radiative exchange in a complex-shaped enclosure composed of solid spherical surfaces, two horizontal imaginary transparent planes at the top and at the bottom, and four vertical imaginary specularly reflecting planes with unity reflectivity [19]. Obviously, the apparent transmissivity and the apparent reflectivity of the packed system are equivalent to the incident radiative transfer rates of the bottom and the top imaginary surfaces, respectively.

We first solve the apparent transmissivity T_r and the apparent reflectivity R_f of the packed sphere system by the successive approximation method. Since the geometry of the system is very complicated, the RMC with importance sampling is preferable and is adopted. Comparing the present direct results with those solved by the discrete-ordinates method developed in [19], we find that they are in very good agreement for either diffuse or specular reflecting.

Then, we consider the inverse problem estimating the surface reflectivity of the spheres from T_r or from R_f of the packed system. The inverted results for diffuse and specular cases from the 'measured' T_rs and the 'measured' R_fs reported in [19] are listed in the top half of Table 3, respectively. The effects of measurement error on inverted results are also considered. We use the values of T_r and R_f obtained by adding or subtracting 1.0 and 3.0% of the solutions reported in [19] as the measured values, and the inverted results are tabulated in the bottom half of Table 3.

The inverted results with zero simulated measurement error agree very well with the exact values except for those determined from T_r for a small ρ_d or ρ_s, as shown in the top half of Table 3. The reason of the worse results for small ρ_d or ρ_s is the same as that of the worse results for the above cylindrical channel example with small ρ_d or ρ_s. As shown in the bottom half of Table 3, the larger simulated measurement errors induce larger deviations from the exact values, and the present technique can still generate meaningful results even for the cases with 3.0% simulated measurement error except the results inverted from T_r for $\rho_d = 0.1$ or $\rho_s = 0.1$. Since great progress of the measurement technique of the hemi-spherical reflectivity of a surface for diffuse irradiation has been made [20], estimating the surface reflectivity of the spheres from R_f seems superior to that from T_r in the packed sphere system.

The present inverse method requires 135 CPU s on a HP 715 workstation to determine three values of specular sphere surface reflectivity in a three-layered system employing 500 000 bundles.

4.3. Radiative transfer from an infinite plane to rows of parallel tubes of infinite length

In the third example, we consider rows of parallel tubes arranged between two parallel infinite transparent planes, and the top plane is exposed to an external radiation equal to the emissive power of a black surface E_b. Each row consists of infinitely many tubes of infinite length and diameter D arranged in an equal center-to-center distance C, and the separation distance between two adjacent rows is H. To illustrate, a system of three rows is shown in Fig. 2(c). The tubes are assumed to be identical, uniform, cold, absorbing, and diffusely reflecting with the surface reflectivity ρ_d. Since the considered two-dimensional system extends to infinity in the direction parallel to the top and bottom planes, we can consider only a column confined by two 'symmetrical' planes which can be treated as specularly reflecting surfaces of unit reflectivity, as shown in Fig. 2(c).

To treat the complicated geometry of the system, the RMC with importance sampling is adopted. The view factors from an emitting black top plane to each row in a ten-tube-row configuration with rows arranged in an equilateral triangular array ($H = (\sqrt{3}C)/2$) has been obtained recently [21] by a conventional Monte Carlo method. For comparison purpose, we applied the present technique to the same computation by using 10 000 000 bundles, and set $\rho_d = 0$ in the algebraic expression developed, since the tube surfaces considered in [21] are assumed to be black. Comparison of the present results and those obtained by [21] shows that they are the same to the four digits.

Then, the present bundle-tracing code is applied to the diffusely reflecting cases consisting of two rows of tubes; the reflectivities of tube surfaces of the first and the second rows are ρ_{d1} and ρ_{d2}, respectively. The top half of Table 4 lists the apparent transmissivity T_r and the apparent reflectivity R_f obtained for the two-row system exposed to diffuse radiation. From the top half of Table 4, we find that the performance of the RMC is better for a tube with a larger reflectivity and the piece-wise constant reflectivity

Table 3
The inverted diffuse and specular surface reflectivities of spheres in three-layer packed sphere systems from T_r or R_f with or without simulated measurement errors

			Inverted from T_r	Inverted from R_f
ρ_d	T_r [19]	R_f [19]	$\hat{\rho}_d$	
0.1	0.0021	0.0619	0.1430 (0.0603)	0.0998 (0.0002)
0.5	0.0032	0.3466	0.5122 (0.0123)	0.4992 (0.0007)
0.9	0.0150	0.7635	0.9022 (0.0010)	0.8992 (0.0008)
ρ_s	T_r [19]	R_f [19]	$\hat{\rho}_s$	
0.1	0.0024	0.0498	0.0955 (0.0145)	0.1001 (0.0002)
0.5	0.0061	0.2978	0.4961 (0.0043)	0.5002 (0.0007)
0.9	0.0371	0.7162	0.8997 (0.0008)	0.9002 (0.0007)
ρ_d	Measurement error		$\hat{\rho}_d$	
0.1	−3.0%		0.0771 (0.0810)	0.0969 (0.0002)
	−1.0%		0.1231 (0.0658)	0.0988 (0.0002)
	+1.0%		0.1612 (0.0558)	0.1008 (0.0002)
	+3.0%		0.1940 (0.0486)	0.1027 (0.0002)
0.5	−3.0%		0.4950 (0.0134)	0.4863 (0.0007)
	−1.0%		0.5067 (0.0127)	0.4949 (0.0007)
	+1.0%		0.5177 (0.0120)	0.5034 (0.0007)
	+3.0%		0.5280 (0.0114)	0.5119 (0.0007)
0.9	−3.0%		0.8986 (0.0010)	0.8833 (0.0008)
	−1.0%		0.9011 (0.0010)	0.8940 (0.0008)
	+1.0%		0.9034 (0.0010)	0.9044 (0.0008)
	+3.0%		0.9057 (0.0010)	0.9145 (0.0008)
ρ_s	Measurement error		$\hat{\rho}_s$	
0.1	−3.0%		0.0792 (0.0152)	0.0972 (0.0002)
	−1.0%		0.0909 (0.0147)	0.0991 (0.0002)
	+1.0%		0.1000 (0.0144)	0.1011 (0.0002)
	+3.0%		0.1110 (0.0139)	0.1030 (0.0002)
0.5	−3.0%		0.4862 (0.0045)	0.4882 (0.0007)
	−1.0%		0.4929 (0.0044)	0.4962 (0.0007)
	+1.0%		0.4993 (0.0043)	0.5041 (0.0007)
	+3.0%		0.5056 (0.0042)	0.5119 (0.0007)
0.9	−3.0%		0.8953 (0.0008)	0.8862 (0.0007)
	−1.0%		0.8982 (0.0008)	0.8956 (0.0007)
	+1.0%		0.9011 (0.0008)	0.9047 (0.0007)
	+3.0%		0.9039 (0.0008)	0.9136 (0.0007)

($W/D = 1.1547$, $N = 500\,000$).

does not seem to induce any particular difficulty. However, a little bit larger computer memory is required to store the values of the coefficients in the algebraic expression generated by the successive approximation.

Finally, we consider the inverse problem estimating the surface reflectivities of the tubes in a two-row system exposed to diffuse radiation. We first develop the two algebraic equations in terms of the two unknown surface reflectivities by the present technique. Giving 'measured' T_r and R_f and solving the two algebraic equations sim-

Table 4
The direct results of T_r and R_f and the inverted diffuse surface reflectivities of tubes in a 2-tube-row configuration from T_r and R_f with simulated measurement errors

ρ_{d1}	ρ_{d2}	R_f	T_r
0.2	0.2	0.1142 (0.00003)	0.1543 (0.00011)
0.5	0.5	0.3011 (0.00007)	0.1751 (0.00011)
0.8	0.8	0.5221 (0.00011)	0.2218 (0.00012)
0.2	0.5	0.1323 (0.00004)	0.1622 (0.00011)
0.5	0.2	0.2785 (0.00007)	0.1622 (0.00011)
0.2	0.8	0.1522 (0.00006)	0.1729 (0.00011)
0.8	0.2	0.4553 (0.00012)	0.1728 (0.00011)
0.5	0.8	0.3275 (0.00008)	0.1929 (0.00011)
0.8	0.5	0.4848 (0.00011)	0.1929 (0.00011)

ρ_{d1}	ρ_{d2}	Measurement error	$\hat{\rho}_{d1}$	$\hat{\rho}_{d2}$
0.2	0.5	−2.0%	0.2092 (0.0036)	0.3774 (0.0041)
		−1.0%	0.2045 (0.0033)	0.4402 (0.0039)
		+1.0%	0.1958 (0.0028)	0.5571 (0.0036)
		+2.0%	0.1918 (0.0026)	0.6115 (0.0034)
0.5	0.2	−2.0%	0.5015 (0.0044)	0.1071 (0.0035)
		−1.0%	0.5007 (0.0040)	0.1546 (0.0033)
		+1.0%	0.4995 (0.0034)	0.2434 (0.0031)
		+2.0%	0.4991 (0.0032)	0.2850 (0.0030)
0.5	0.5	−2.0%	0.4995 (0.0025)	0.4279 (0.0026)
		−1.0%	0.4997 (0.0024)	0.4647 (0.0025)
		+1.0%	0.5004 (0.0021)	0.5339 (0.0023)
		+2.0%	0.5009 (0.0020)	0.5665 (0.0023)
0.5	0.8	−2.0%	0.4977 (0.0016)	0.7454 (0.0019)
		−1.0%	0.4988 (0.0015)	0.7732 (0.0019)
		+1.0%	0.5013 (0.0014)	0.8258 (0.0018)
		+2.0%	0.5026 (0.0014)	0.8506 (0.0018)
0.8	0.5	−2.0%	0.7921 (0.0018)	0.4566 (0.0019)
		−1.0%	0.7960 (0.0017)	0.4787 (0.0018)
		+1.0%	0.8040 (0.0016)	0.5204 (0.0017)
		+2.0%	0.8081 (0.0015)	0.5400 (0.0017)
0.8	0.8	−2.0%	0.7908 (0.0011)	0.7701 (0.0013)
		−1.0%	0.7954 (0.0011)	0.7854 (0.0013)
		+1.0%	0.8046 (0.0010)	0.8140 (0.0013)
		+2.0%	0.8093 (0.0010)	0.8275 (0.0012)

$C/D = 2.0$, $H/D = 1.732$.

ultaneously, we can obtain ρ_{d1} and ρ_{d2}. Some inverted results are shown in the bottom half of Table 4.

Since no other direct solution of high order accuracy seems to be available, we employ the direct solutions listed in the top half of Table 4 and put more emphasis on the effects of measurement errors on the inverted results. The tabulated results are obtained by the present method for various values of simulated measurement errors. Here, we add or subtract 1.0 or 2.0% of the direct solutions of T_r and R_f simultaneously as the 'measured' values. From the bottom half of Table 4, the discrepancy between the inverted and the exact values decreases as the simulated measurement errors become small, as expected, and the surface reflectivity of the second row is more

sensitive to the measurement errors than that of the first row. In other words, the estimation of the surface reflectivity of the first row is easier than that of the second row. Moreover, the effects of measurement errors on the inverted results are pronounced when the surface reflectivity is small.

The CPU time required to estimate 24 sets of the two surface reflectivities using 10 000 000 bundles on a HP 715 workstation is about 1600 s. The bundle-tracing procedure of the RMC uses most of the CPU time.

5. Concluding remarks

In the above exemplifications, a technique based on successive approximation is adopted to solve direct and inverse problems of radiative exchange among surfaces. In the solution procedure of the direct problems, either the RMC with importance sampling or the QM is employed only once to obtain the expression of solutions for various surface reflectivities, provided that the geometry and the driving term are fixed. Therefore, the present technique can save the computational labor when a large number of cases with different values of reflectivities are studied for the same geometry. Comparisons of the present results of direct problems and the results available in the literature show excellent agreement.

Similarly, when one applies the present technique to an inverse problem estimating the surface reflectivities, one does not need to solve the associated direct problem repetitively. As the examples shown, from the knowledge of the geometrical configuration and the incident radiative transfer rates of surfaces, including the apparent transmissivity or reflectivity of a system exposed to external radiation, we can estimate the surface reflectivities efficiently. The inverted results are in good agreement with the exact values. The present technique can still generate meaningful results even for the cases with 3.0% simulated measurement error except the results inverted from the apparent transmissivity of a system with very small reflectivity. The required CPU time is far less than that for using an iterative algorithm with a conventional Monte Carlo method to solve direct radiative exchange.

Acknowledgement

This work was supported in part by the National Science Council of the Republic of China in Taiwan through Grant NSC 83-0401-E-006-111.

Appendix

In this Appendix, we show that equation (4), in essence, is a Fredholm integral equation of the second kind where I is the unknown, $\bar{r}$ is the independent variable and $\hat{s}$ is a parameter. First, we express equation (4) in the surface integral form

$$I(\bar{r},\hat{s}) = V(\bar{r},\hat{s}) + \int_A \rho''(\bar{r},\hat{s}',\hat{s}) c_v(\bar{r}';\bar{r}) I(\bar{r}',\hat{s}') \frac{\mu_i \mu'}{|\bar{r}-\bar{r}'|^2} \mathrm{d}A' \tag{A1}$$

where $\hat{s}'$ is expressed by $\bar{r}$, $\bar{r}'$

$$\hat{s}' = \frac{\bar{r}-\bar{r}'}{|\bar{r}-\bar{r}'|} \tag{A2}$$

Both $\bar{r}$ and $\bar{r}'$are on the enclosure surface described by a function

$$g(\bar{r}) = 0 \tag{A3}$$

The unit normal vector $\hat{n}$ of $\mathrm{d}A$ can be expressed as

$$\hat{n} = \pm \frac{\nabla g(\bar{r})}{|g(\bar{r})|} \tag{A4}$$

The sign in equation (A4) is determined by the requirement that $\hat{n}$ is an inward normal for the volume enclosed by $g(\bar{r}) = 0$. Hence, $\mu_i = (-\hat{s}') \cdot \hat{n}$ and $\mu' = \hat{s}' \cdot \hat{n}'$. Then, equation (A1) can be rewritten as

$$I(\bar{r},\hat{s}) = V(\bar{r},\hat{s}) + \int_A \rho''\left(\bar{r}, \frac{\bar{r}-\bar{r}'}{|\bar{r}-\bar{r}'|}, \hat{s}\right) c_v(\bar{r}';\bar{r}) I\left(\bar{r}, \frac{\bar{r}-\bar{r}'}{|\bar{r}-\bar{r}'|}\right) \times \frac{1}{|\bar{r}-\bar{r}'|^4} (\bar{r}'-\bar{r}) \cdot \left[\pm \frac{\nabla g(\bar{r})}{|\nabla g(\bar{r})|}\right] (\bar{r}-\bar{r}') \cdot \left[\pm \frac{\nabla g(\bar{r}')}{|\nabla g(\bar{r}')|}\right] \mathrm{d}A' \tag{A5}$$

Therefore, the integral equation of intensity is indeed a Fredholm integral equation of the second kind with a parameter $\hat{s}$.

References

[1] R. Siegel, J.R. Howell, Thermal Radiation Heat Transfer, 3rd ed., Hemisphere, New York, 1992, p. 189.
[2] M.F. Modest, Radiative Heat Transfer, 1st ed., McGraw-Hill, New York, 1993, p. 155, p. 214.
[3] T.J. Love, Radiative Heat Transfer, 1st ed., Charles E. Merrill, Columbus, 1968, pp. 58–60.
[4] D.M. O'Brien, Accelerated quasi Monte Carlo integration of the radiative transfer equation, Journal of Quantitative Spectroscopy and Radiative Transfer 48 (1992) 41–59.
[5] D.V. Walters, R.O. Buckius, Monte Carlo methods for radiative heat transfer in scattering media, in: C.L. Tien (Ed.), Annual Review of Heat Transfer, vol. 5, CRC, Boca Raton, 1994, pp. 131–176.
[6] C.T.H. Baker, The Numerical Treatment of Integral Equations, 1st ed., Oxford University Press, Oxford, 1977, p. 375.
[7] W.J. Wu, G.P. Mulholland, Two-dimensional inverse radiation heat transfer analysis using Monte Carlo techniques, Proceedings of the 1989 National Heat Transfer Conference, HTD-vol. 106, ASME, New York, 1989, pp. 181–190.

[8] Ye.K. Belonogov, A.Yu. Zatsepin, Comparative analysis of numerical methods for solving integral equations of inverse problems of radiative heat transfer, Soviet Journal of Applied Physics 3 (1989) 1–11.
[9] Ye.K. Belonogov, I.S. Vinogradov, A.Yu. Zatsepin, Reconstruction of the temperature surface from a given radiation field on another surface, Soviet Journal of Applied Physics 3 (1989) 12–18.
[10] S.P. Rusin, Solution of inverse problems in the design of heating systems by means of opto-geometric functions, Soviet Journal of Applied Physics 3 (1989) 19–25.
[11] M. Oguma, J.R. Howell, Solution of two-dimensional blackbody inverse radiation problem by inverse Monte Carlo method, Proceedings of the ASME/JSME Thermal Engineering Joint Conference, vol. 3, ASME, New York, 1995, pp. 243–250.
[12] V. Harutunian, J.C. Morales, J.R. Howell, Radiation exchange within an enclosure of diffuse-gray surfaces: the inverse problem, Proceedings of the 30th 1995 National Heat Transfer Conference, vol. 10, ASME, New York, 1995, pp. 133–140.
[13] W.-J. Yang, H. Taniguchi, K. Kudo, Radiative heat transfer by the Monte Carlo method, Advances in Heat Transfer, vol. 27, Academic, San Diego, 1995, pp. 86–104.
[14] W.L. Dunn, Inverse Monte Carlo analysis, Journal of Computational Physics 41 (1981) 154–166.
[15] A. Rabl, Radiation transfer through specular passages—a simple approximation, International Journal of Heat and Mass Transfer 20 (1977) 323–330.
[16] W.H. Press, S.A. Teukolsky, W.T. Vetterling, B.P. Flannery, Numerical Recipes in FORTRAN: The Art of Scientific Computing, 2nd ed., Cambridge University Press, New York, 1992, pp. 352–355.
[17] C.K. Chan, C.L. Tien, Radiative transfer in packed spheres, Journal of Heat Transfer 96C (1974) 52–58.
[18] K. Kudo, W.-J. Yang, H. Taniguchi, H. Hayasaka, Radiative heat transfer in packed spheres by Monte Carlo method, in: W.-J. Yang, Y. Mori, (Eds.), Heat Transfer in High Technology and Power Engineering, 1st ed., Hemisphere, New York, 1987, pp. 529–540.
[19] B.-T. Liou, S.-H. Wu, C.-Y. Wu, Radiative heat transfer in a packed bed of diffusely reflecting spheres, Journal of the Chinese Society of Mechanical Engineers/Chung-Kuo Chi Hsueh Kung Ch'eng Hsuebo Pao 16 (1995) 91–97.
[20] T. Makino, T. Yoshida, S. Tanaka, A new reflectometer for measuring the spectrum of hemispherical reflectance for perfect-diffuse hemispherical irradiation, Heat Transfer—Japanese Research 23 (1994) 103–115.
[21] D.L. Qualey, J.R. Welty, M.K. Drost, Monte Carlo simulation of radiation heat transfer from an infinite plane to parallel rows of infinitely long tubes—Hottel extended, Numerical Heat Transfer 31A (1997) 131–142.